Three-dimensional direct femtosecond laser writing of second-order nonlinearities in glass

Jiyeon Choi,[1,2] Matthieu Bellec,[2,*] Arnaud Royon,[2] Kevin Bourhis,[3] Gautier Papon,[2] Thierry Cardinal,[3] Lionel Canioni,[2] and Martin Richardson[1]

[1] *Townes Laser Institute, CREOL, University of Central Florida, Orlando, Florida 32816-2700, USA*

[2] *LOMA—CNRS/University of Bordeaux, 351 Cours de la Libération, 33405 Talence Cedex, France*

[3] *ICMCB—CNRS/University of Bordeaux, 87 Avenue Dr. Schweitzer, 33608 Pessac Cedex, France*

**Corresponding author: bellec@unice.fr*

Received December 5, 2011; revised January 12, 2012; accepted January 12, 2012; posted January 12, 2012 (Doc. ID 158807); published March 8, 2012

We demonstrate that direct femtosecond laser writing in silver-containing zinc and gallium phosphate glass enables generation of three-dimensional (3D) optical second-order nonlinear microstructures having an $\chi^{(2)}$ value about 2.5 times that of quartz. The proposed physical model involves photo-reduction, photo-dissociation, and migration of silver species within the glass matrix. 3D laser-written second-order nonlinear structures could become a new class of nonlinear optical components. © 2012 Optical Society of America

OCIS codes: 190.4400, 160.5335, 160.1245, 140.3390.

Second-order nonlinear optical phenomena such as second-harmonic generation (SHG) and the Pockels effect are widely used in many photonic devices, enabling new laser source wavelengths and the high speed external modulation of light for multiple purposes [1]. These devices are, however, inherently restricted to using noncentrosymmetric materials such as nonlinear optical crystals or poled materials that exhibit second-order nonlinearities [2]. Despite the existence of a number of nonlinear optical crystals and the improving capabilities of poled materials, there are still essential gaps in the range and operability of these devices. Commercial applications relying on the second-order nonlinearity are still limited due to this narrow choice of suitable materials. There is thus a lingering need for a new class of nonlinear optical materials possessing second-order nonlinearities sufficiently large over a wide spectral range.

Glasses have been widely used as optical materials for many applications, in part because of the ease in tailoring their properties by changing their composition. Their remarkable properties, such as good mechanical and chemical durability, allow ease of preparation in various forms, such as fibers and curved substrates [3]. The possibility to incorporate in these vitreous materials noble metal ions allows one to increase their photosensitivity and to access to new or improved optical properties. If one can induce second-order nonlinearity by breaking their centrosymmetry, then perhaps glasses would become promising candidates for second-order nonlinear optical applications.

There are various techniques to break the centrosymmetry. One way is to polarize the glass, the so-called poling process, either optically in optical fibers [4] or thermally [5]. There have been many attempts to produce thermally poled glass systems in silicate [6], tellurite [7], and phosphate [8] matrices. The basic idea of thermal poling is to create a frozen electric field E_{dc} inside a nonlinear layer as an anodic depleted-ion region caused by the localized migration of mobile ions. The interaction between this permanent electric field and the third-order nonlinear susceptibility $\chi^{(3)}$ of the glass gives rise to an effective second-order nonlinear response $\chi^{(2)}_{eff} = 3\chi^{(3)}E_{dc}$, the well-known electric field-induced second-harmonic generation (EFISHG) effect.

Femtosecond laser direct writing is a technique that can be utilized in transparent materials to fabricate microstructures in three dimensions with modified physical properties thanks to multiphoton absorption [9]. This technique can be applied to induce localized second-order nonlinearities in glass, either by changing the crystalline phase from amorphous into crystallite [10,11], or by modifying the morphology of metal nanoparticles embedded in glass from spherical to ellipsoidal [12].

In this Letter, we propose another approach to create inside a silver-containing zinc phosphate glass a laser-induced frozen charge gradient, similar to the thermal poling process, but localized with three-dimensionality. We show that the inhomogeneous charge distribution produced in the laser-exposed glass can give rise to a second-order nonlinearity that can be exploited for nonlinear optical applications. We suggest a model for this process and demonstrate SHG from a silver microstructure to prove the concept. The polarization of the SHG is analyzed to confirm the theoretical EFISHG model. Finally, the SHG efficiency of a silver microstructure is compared to quartz to estimate the induced $\chi^{(2)}_{eff}$.

The glass used for this study is a photosensitive zinc and gallium phosphate glass ($40P_2O_5 - 55ZnO - 4Ga_2O_3 - 1Ag_2O$) containing 1% (mol.%) of silver oxyde. Details of the glass fabrication process and the material properties are described elsewhere [13]. A Yb-doped fiber 450 fs ultrafast laser (μJewel, IMRA America Inc.) operating at 1045 nm with a repetition rate of 1.5 MHz and a maximum pulse energy of 200 nJ was used for the irradiation.

0146-9592/12/061029-03$15.00/0

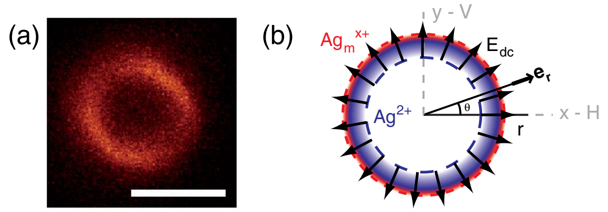

Fig. 1. (Color online) (a) Confocal fluorescence image of a photo-induced ring structure with an excitation at 405 nm. The scale bar is 5 μm. (b) Schematic representation of a possible radial distribution of the silver species inside the ring. The permanent electric field is E_{dc}.

A microscope objective ($\mathrm{NA} = 0.25$) focused the laser beam into the glass sample mounted on a computer controlled three-dimensional (3D) stage. Silver microstructures consisting of fluorescent silver clusters $\mathrm{Ag}_m^{x+}(m < 10)$ were created by irradiating the samples for 1 second at an irradiance of 5.6 TW.cm^{-2} in a 4 μm diameter spot. The key mechanisms contributing to this clustering is a combination of photo-reduction ($2\mathrm{Ag}^+ \rightarrow \mathrm{Ag}^0 + \mathrm{Ag}^{2+}$), photo-dissociation, and thermal and chemical diffusions, due to heat accumulation resulting from the high repetition rate laser pulses [14,15]. As a result, these fluorescent clusters are arranged into a ring shape in 2D (see Fig. 1(a)), a pipe shape in 3D. Figure 1(b) depicts schematically and hypothetically the laser-induced distribution of the silver species. Permanent static electric fields with circular symmetry are formed between the hole-trap color centers, such as Ag^{2+} located inside the rim and the electron-trap silver clusters Ag_m^{x+} situated on the outside of the rim of the microstructure [15]. Although the spatial distribution of the silver species is clearly radial, their exact repartition inside the ring in not yet known and needs to be measured by near-field experiments.

Treating this polled structure as a nonlinear medium irradiated now by a probe beam E_{probe} of angular frequency ω, the induced second-order polarization in the structure depicted in Fig. 1(a) can be represented as decomposed forms in x and y [2]:

$$P_x(2\omega) = 3\varepsilon_0 \chi^{(3)}_{xxxx} E^2_{\mathrm{probe\_}x}(E_{\mathrm{dc}} \cos\theta),$$
$$P_y(2\omega) = 3\varepsilon_0 \chi^{(3)}_{yxxy} E^2_{\mathrm{probe\_}x}(E_{\mathrm{dc}} \sin\theta), \qquad (1)$$

where θ is the angle between an electric field vector and the polarization of the probe beam. P_x and P_y represent the polarizations along the x (horizontal, H) and y (vertical, V) axes. The probe beam $E_{\mathrm{probe\_}x}$ is polarized along the x-direction. The second-harmonic (SH) irradiances associated to the above second-order polarizations are given by

$$I_{\mathrm{HH}}(2\omega) \propto |\chi^{(3)}_{xxxx}|^2 |E^2_{\mathrm{probe\_}x}|^2 |E_{\mathrm{dc}}|^2 |\cos\theta|^2,$$
$$I_{\mathrm{HV}}(2\omega) \propto |\chi^{(3)}_{yxxy}|^2 |E^2_{\mathrm{probe\_}x}|^2 |E_{\mathrm{dc}}|^2 |\sin\theta|^2. \qquad (2)$$

The SHG measurements were performed with the same laser (see Fig. 2(a)), but with a power reduced by ~57% of the power needed for structuring of the material. The SH signal from the structured sample was collected

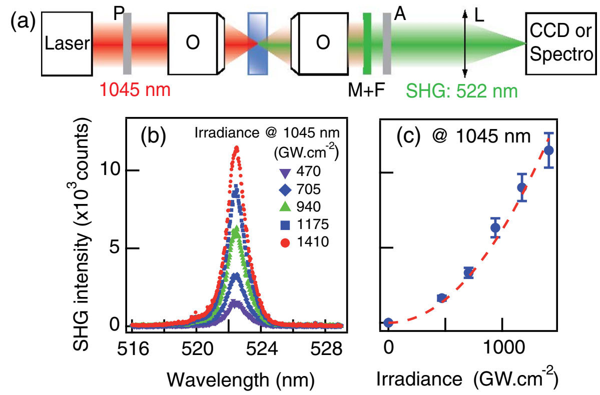

Fig. 2. (Color online) (a) Experimental setup for SH observation of a single ring microstructure (P: polarizer, O: microscope objective, M: dichroic mirror HR IR, F: bandpass filter at 522 nm $\pm$ 40 nm, A: analyzer, L: lens). (b) SH spectra at different probe irradiances of the fundamental beam. (c) Evolution of the SH intensity versus the irradiance of the fundamental beam. The quadratic evolution is respected, evidencing the SHG process.

through a microscope objective ($\mathrm{NA} = 0.4$) and a set of filters. The SH signal was coupled into an intensified CCD (ICCD) camera attached to a spectrometer via a fiber-optic delivery. A CCD beam profiler was used to visualize the SHG distribution. A polarizer was located in front of the CCD beam profiler to analyze the polarization dependence of SH signal. The presence of SHG was confirmed by the spectral line centered at 522 nm for different probe irradiances (Fig. 2(b)) and by the quadratic dependence of the SH intensity relative to the fundamental irradiance (Fig. 2(c)).

Figure 3 shows the experimental and theoretical derived images of the SH signal for parallel (*HH* in Fig. 3(a) and (c)) and crossed (*HV* in Fig. 3(b) and (d)) polarizers and analyzers. The experimental images show a central spot encircled by two meniscal lobes with a scale corresponding to what we believe to be the nonlinear region formed by the space charge distribution. Figure 3(e) represents the evolution of the SH intensity

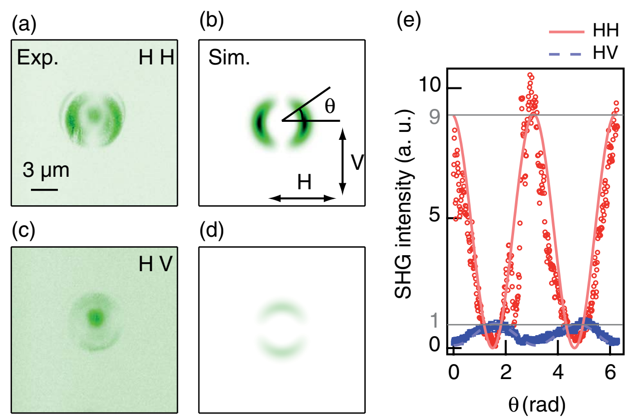

Fig. 3. (Color online) Experimental and associated theoretical images of the SH signal for parallel *HH* (a),(c) and crossed *HV* (b),(d) polarizers and analyzers. (e) Evolution of the SH intensity versus the angle of the electric field vector for parallel (*HH*) and crossed (*HV*) polarizers and analyzers.

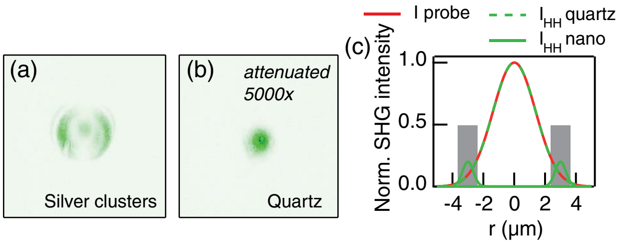

Fig. 4. (Color online) Experimental images of the SH signal for a parallel HH polarizer and analyzer of a (a) single ring structure and of (b) bulk quartz attenuated 5000 times. (c) Evolution of the normalized SH intensity of the ring structure (green full line) and of bulk quartz (green dotted line) versus the radial coordinate. The gray zones correspond to the integration areas where the $\chi^{(2)}$ of the ring is measured.

versus the angle of the electric field vector for parallel (HH) and crossed (HV) polarizers and analyzers. As expected, the ratio of the intensity maxima for each polarization is $I_{HH}^{\max}:I_{HV}^{\max} = 9:1$ for horizontal and vertical directions, as given by the Kleinmann symmetry relation $\chi_{xxxx}^{(3)}:3\chi_{yxxy}^{(3)} = 3:1$ in glass [2]. The theory is in good agreement with the experimental images, except for the central region where a signal is observed. This signal seems to be insensitive to the analyzer orientation and is quite directional. The physical origin of this signal is not clear and is still under investigation. It could be due to a pump leakage, a contribution of the longitudinal component of the focused beam, a guiding effect that depolarizes the SH signal, or the 3D organization of the structure (pipe), which is not taken into account in our 2D model (ring).

Finally, in order to estimate the SHG efficiency of this microstructure, it was compared with that of z-cut quartz and normalized to the SH intensity of the quartz crystal exposed to the same probe irradiance (Fig. 4). The estimated $\chi_{\rm eff}^{(2)}$ is 2.5 that of quartz, corresponding to $\sim$1.2 pm.V^{-1}. Thus the laser-induced value of $\chi^{(2)}$ is comparable to that achieved with thermal poling of glass of similar composition, i.e., $\sim$1.8 pm.V^{-1} [16]. The third-order susceptibility of the silver-containing zinc phosphate glass is of the same order of magnitude as that of fused silica, i.e., $\chi^{(3)} = 2.5 \times 10^{-22}$ m^2.V^{-2}. The internal electric field can therefore be estimated to be $\sim 1.6 \times 10^9$ V.m^{-1}. This value is extremely large and is close to the electric field of an electron-ion dipole in an atom. Note that one possibility to get a higher $\chi_{\rm eff}^{(2)}$ value could be to modify the glass composition and the introduction of hyperpolarizable ions in order to increase the third-order nonlinearity of the material.

In conclusion, we have proposed and demonstrated a new method based on femtosecond laser-induced depletion to create high second-order nonlinear optical properties in silver-containing photosensitive glass. This nonlinearity was produced in μm-scale structures, consisting of charged silver clusters, inducing an inhomogeneous space charged distribution with an associated permanent static electric field. We have estimated the induced second-order susceptibility of these structures to be $\sim$2.5 times that of quartz. This new laser-based method of creating new nonlinear optical materials opens a new pathway in the development of active and nonlinear optical components. Moreover, since this laser writing method allows for the micron-scale structuring of this nonlinearity in precision-designed 3D configurations, it opens the door to the development of many new classes of optical systems and components including multifunctional lab-on-chip devices, active 3D optical storage devices [13], and high damage threshold optical converters.

The authors acknowledge the Conseil Régional d'Aquitaine, the GIS AMA, and the ANR (grant 2010 BLAN 946 03) for their financial support, as well as P. Legros and the BIC for the confocal fluorescence microscopy images.

References

1. B. E. A. Saleh and M. C. Teich, *Fundamentals of Photonics* (Wiley, 1991).
2. R. W. Boyd, *Nonlinear Optics*, 3rd ed. (Academic Press, 2008).
3. J. Zarzycki, *Glasses and the Vitreous State* (Cambridge University, 1991), Vol. **9**.
4. U. Österberg and W. Margulis, Opt. Lett. **11**, 516 (1986).
5. R. Myers, N. Mukherjee, and S. Brueck, Opt. Lett. **16**, 1732 (1991).
6. P. Kazansky, A. Smith, P. Russell, G. Yang, and G. Sessler, Appl. Phys. Lett. **68**, 269 (1996).
7. K. Tanaka, K. Kashima, K. Hirao, N. Soga, A. Mito, and H. Nasu, Jpn. J. Appl. Phys. **32**, L843 (1993).
8. M. Dussauze, E. Fargin, V. Rodriguez, A. Malakho, and E. Kamitsos, J. Appl. Phys. **101**, 083532 (2007).
9. A. Royon, Y. Petit, G. Papon, M. Richardson, and L. Canioni, Opt. Mat. Exp. **1**, 866 (2011).
10. K. Miura, J. Qiu, T. Mitsuyu, and K. Hirao, Opt. Lett. **25**, 408 (2000).
11. Y. Dai, B. Zhu, J. Qiu, H. Ma, B. Lu, and B. Yu, Chem. Phys. Lett. **443**, 253 (2007).
12. A. Podlipensky, J. Lange, G. Seifert, H. Graener, and I. Cravetchi, Opt. Lett. **28**, 716 (2003).
13. L. Canioni, M. Bellec, A. Royon, B. Bousquet, and T. Cardinal, Opt. Lett. **33**, 360 (2008).
14. M. Bellec, A. Royon, B. Bousquet, K. Bourhis, M. Treguer, T. Cardinal, M. Richardson, and L. Canioni, Opt. Express **17**, 10304 (2009).
15. M. Bellec, A. Royon, K. Bourhis, J. Choi, B. Bousquet, M. Treguer, T. Cardinal, J.-J. Videau, M. Richardson, and L. Canioni, J. Phys. Chem. C **114**, 15584 (2010).
16. M. Dussauze, E. Kamitsos, E. Fargin, and V. Rodriguez, J. Phys. Chem. C **111**, 14560 (2007).